Electrochimica Acta 54 (2009) 3589–3593

Contents lists available at ScienceDirect

Electrochimica Acta

journal homepage: www.elsevier.com/locate/electacta

Electrochemical oxidation of oxalate ion in the presence of fluoride ion, and radical analysis by ESR

Shuhuan Li [a], Art van der Est [b], Nigel J. Bunce [a,*]

[a] Department of Chemistry, University of Guelph, 50 Stone Road East, Guelph, Ontario, Canada N1G 2W1
[b] Department of Chemistry, Brock University, 500 Glenridge Ave, St. Catharines, Ontario, Canada L2S 3A1

ARTICLE INFO

Article history:
Received 15 September 2008
Received in revised form 6 January 2009
Accepted 11 January 2009
Available online 19 January 2009

Keywords:
Spin trap
Electron spin resonance
α-(4-pyridyl-1-oxide) N-tert-butyl-nitrone (POBN)
Oxalate
Electrochemical oxidation
Hydroxyfluoride radical anion

ABSTRACT

The problem at hand is the electrochemical oxidation of oxalate ion, which is accelerated by fluoride ion at a platinum anode. The hypothesis that fluoride ion traps incipient hydroxyl radicals as hydroxyfluoride radical anions was not supported by ESR experiments in which hydroxyl radicals were generated in the presence of the spin trap α-(4-pyridyl-1-oxide) N-*tert*-butyl-nitrone with and without the addition of fluoride ion. The electrochemical oxidation of oxalate at constant current followed current controlled kinetics both at a platinum anode, as observed previously, and at a boron-doped diamond anode, but the rate of the latter reaction was indifferent to the presence of fluoride ion. We propose that the competition of fluoride and hydroxide ions for the Pt/PtO_n surface inhibits the dimerization reactions that lead to oxygen evolution; the displacement of oxygen evolution to more positive potentials overcomes the overpotential for the oxidation of oxalate at this anode. Fluoride ion has no influence on the oxidation of oxalate at BDD because oxygen evolution inherently occurs at more positive potentials at this anode.

1. Introduction

Low molecular weight aliphatic acids are the penultimate products in the electrochemical mineralization of organic contaminants (e.g., [1–3]), and as a result many studies of their electrochemical oxidation have been reported (e.g., [4–9]). In particular, oxalic acid is recognized as being rather recalcitrant towards oxidation to CO_2 [10–13].

The present study was stimulated by a report by Martínez-Huitle et al. [14] on the electrochemical oxidation of oxalate at a Pt anode in the presence of halide ions in alkaline media (Na_2SO_4 + NaOH as supporting electrolyte). Mineralization occurred by mass transfer limited kinetics (first-order in oxalate), according to Fig. 5 of the cited work. Addition of halide salts increased the rate of mineralization in the order: control < NaCl < NaBr < NaF. The authors postulated that with NaCl and NaBr the electrochemical oxidation was mediated by oxyanion species (hypohalites) [14,15]; this explanation is untenable for fluoride ion, which does not oxidize to hypofluorite. Voltammetric oxidation curves for oxalate in Na_2SO_4/NaOH/NaF mixtures shifted progressively to more anodic potentials as the concentration of NaF increased (0–0.7 M).

Although the addition of fluoride ion is not practical for the remediation of wastewater, we were intrigued by the ability of fluoride to accelerate the electrochemical oxidation of oxalate. We considered whether F^- might trap the incipient products of water oxidation to form the hydroxyfluoride anion radical ($[F\cdots H{-}O]^{\bullet -}$), which could act as the proximate oxidant for oxalate. The gas-phase analog has been observed by photoelectron spectroscopy [16], and is stable with respect to dissociation into either $OH^\bullet + F^-$ or $OH^- + F^\bullet$ [17]. We used ESR to search for evidence to support the intermediacy of $[F\cdots H{-}O]^{\bullet -}$ and compared the effect of added fluoride in the electrochemical oxidation of oxalate at Pt and boron-doped diamond (BDD) anodes. The results suggested that the enhanced reactivity of oxalate at the Pt anode in the presence of fluoride ion is caused by shifting the oxygen evolution reaction (OER) to more positive potentials.

2. Materials and methods

2.1. Materials

Oxalic acid, iron(II) sulfate heptahydrate, 30% hydrogen peroxide, potassium fluoride dihydrate, potassium dihydrogen phosphate, sodium hydroxide, and anhydrous sodium sulfate were

* Corresponding author. Tel.: +1 519 824 4120x53962; fax: +1 519 766 1499.
E-mail address: nbunce@uoguelph.ca (N.J. Bunce).

0013-4686/$ – see front matter © 2009 Elsevier Ltd. All rights reserved.
doi:10.1016/j.electacta.2009.01.025

obtained from Sigma–Aldrich (Oakville, ON). α-(4-Pyridyl-1-oxide) N-*tert*-butyl-nitrone (POBN) was supplied by Alexis Biochemicals (San Diego, CA).

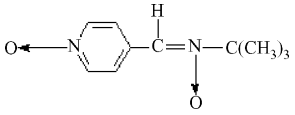

4-POBN

Anode materials comprised a Pt plate of area of 4 cm^2 and boron-doped diamond electrodes (Si/BDD) (including electrolysis anode of 3.5 cm^2 and working electrode of 1 cm^2 supplied by Swiss Center for Electronics and Microtechnology Inc., Neuchâtel. A Pt wire supplied from Sigma–Aldrich (Oakville, ON), with exposed area about 16 mm^2 ($=\pi dh \approx 3.14 \times 0.25\,mm \times 20\,mm$) was used as the counter electrode in cyclic voltammetry. The cathode material for the electrolyses was a stainless steel plate purchased from Electrosynthesis Company (Lancaster, NY). A Hg/Hg_2SO_4 reference electrode (Radiometer Analytical SAS, Lyon, France) was used to monitor the anodic potential during the batch cell electrolyses ($E_{Hg/Hg_2SO_4} = 0.65\,V$ vs. SHE).

2.2. Radical detection

A Bruker model E580 ELEXSYS spectrometer was used for ESR analysis. All experiments were carried out at room temperature. The microwave power was 20 dB; modulation amplitude 1 G, time constant 1.2 ms, conversion time 5.2 ms, sweep time 5.24 s. WinSim 2002, from Public Electron Paramagnetic Resonance Software Tools, was used for ESR spectral simulation.

2.2.1. Fenton generation of hydroxyl radicals

Hydroxyl radicals were chemically generated by mixing H_2O_2 (50 mM) and $FeSO_4{\cdot}7H_2O$ (100 mM) and trapped with 4-POBN (100 mM) in an aqueous buffer solution of potassium dihydrogen phosphate buffer solution (pH 6.0), prepared by partial neutralization of KH_2PO_4.

2.2.2. Photolytic generation of hydroxyl radicals

This method is modified from Janzen et al. [18]. The premixed solution of the spin trap (0.01 M), potassium phosphate buffer (0.05 M at pH 6.0) and hydrogen peroxide (0.3 M) was carefully added into a flat cell positioned in the cavity of ESR spectrometer. A short period of photolysis (2 min) from a Oriel 4.2 W low pressure mercury lamp produced the hydroxyl adduct of the spin trap.

2.3. Electrolyses

Cyclic voltammograms were performed with an EG&G Model 273 potentiostat/galvanostat. Batch electrolyses were performed using a home-built Plexiglas undivided reactor with external dimensions 48 mm × 56 mm × 42 mm and internal dimension 36 mm × 50 mm × 30 mm. The areas of the stainless steel cathode and the BDD anode were 350 mm^2; that of the Pt anode was 4 cm^2. Solutions were stirred during electrolyses using a Thermix stirrer (Fisher Scientific Model 120 MR). Power was supplied by an EG&G Model 363 potentiostat/galvanostat. The cell voltage was monitored using a Wavetek DM5XL voltmeter. The analyte (40 mL) was a 0.1 M solution of oxalic acid in 0.25 M NaOH + 0.50 M Na_2SO_4 (pH > 13) which was used as supporting electrolyte for all electrolyses. Electrolyses were run galvanostatically at 400 or 800 mA; total electrolysis times at BDD ranged from 60 to 90 min and at Pt from 30 to 90 min. To investigate the role of fluoride, the anodic oxidation of oxalate was also carried out in the presence of 0.1 M or 1.0 M KF.

2.4. Analysis

Electrolyses were followed by HPLC, which employed a Waters 600E system, equipped with Waters 2487 dual λ absorbance detector set at 215 nm and a Supelco Discovery C_{18} column 150 mm × 4.6 mm (5 μm), equipped with a silica pre-column guard. The mobile phase was 1:1 methanol: water (filtered through a 0.2 μm filter) at flow rates of 1.0 mL min^{-1} (retention time of oxalate was ~2 min). Calibration samples and electrolysis samples were manually injected with a 150 μL syringe into the 20 μL sample loop of a Rheodyne injector. The chromatograms were evaluated using MassLynx® Version 4.0 software.

X-ray photoelectron spectroscopy was carried out using a Kratos Axis Nova X-ray photo-electron spectrometer at the University of Western Ontario. The survey spectrum was obtained from a ~300 μm × 700 μm area using an Al monochromatic X-ray source. The pass energy for the detector was 160 eV.

3. Results and discussion

3.1. ESR studies

We first sought evidence concerning the existence of the hydroxyfluoride radical anion in solution. Its presumed precursor, the hydroxyl radical, is too reactive to observe directly by ESR, but can be trapped by various spin-trapping agents such as α-(N′-oxido-4-pyridyl)-N-tert.butyl nitrone, whose HO-POBN• spin adduct (**1**) has a well-defined spectrum consisting of a triplet of doublets with a_N = 14.97 G and $a_{H,\beta}$ = 1.68 G [19]. We therefore set out to determine whether it was possible either to trap the hydroxyl radical with fluoride ion and observe the spin adduct $[F\cdots H{-}O]^{\bullet-}$ directly or, if $[F\cdots H{-}O]^{\bullet-}$ were not observable, whether competition between fluoride ion and POBN would decrease the intensity of the HO-POBN• spectrum.

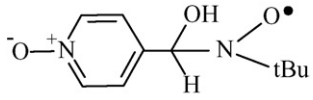

1

Hydroxyl radicals were generated by the Fenton reaction and trapped by POBN to give the expected reference spectrum of HO-POBN• with a_N = 14.89 G and $a_{H,\beta}$ = 1.61 G, along with a small hyperfine splitting from the γ (OH) proton of 0.25 G. This spectrum was simulated using the software WinSim 2002 [20] with parameters a_N = 14.87 G, $a_{H,\beta}$ = 1.67 G, and $a_{H,\gamma}$ = 0.32 G (Supplementary Fig. S1).

When the spectrum was run in the presence of increasing concentrations of fluoride ion the pattern changed progressively. At 0.05 and 0.5 M fluoride ion the spectrum of the HO-POBN• spin adduct was accompanied by spectra that we attributed to spin adducts with one (or two) fluorine substituents at the two (and six) positions of the pyridyl ring, but these did not shed any light on the problem at hand. These spectra, and their simulations, are therefore relegated to the Supplementary Information. At and above 1 M fluoride ion, the HO-POBN• spin adduct was no longer observed, but the spectrum included a wide-spaced doublet of doublets having *a* values 29 and 14 G, corresponding to two nuclei of $I = \pm½$ but no ^{14}N nucleus. Although this might perhaps be attributable to $[F\cdots H{-}O]^{\bullet-}$ we could not confirm this assignment when hydroxyl radicals were generated by photolysis of H_2O_2. Instead, the intensity of the HO-POBN• spectrum decreased monotonically with the concentration of F^-; although this provided indirect evidence for an interaction between HO• and F^- as shown by the kinetic analysis of Scheme 1, it did not explicitly support the production of $[F\cdots H{-}O]^{\bullet-}$.